Surface Science 195 (1988) 353–370
North-Holland, Amsterdam

REGISTRY EFFECTS IN THE THERMODYNAMIC QUANTITIES OF Xe ADSORPTION ON Pt(111)

Klaus KERN, Rudolf DAVID, Peter ZEPPENFELD and George COMSA

Institut für Grenzflächenforschung und Vakuumphysik, Kernforschungsanlage Jülich, Postfach 1913, D-5170 Jülich, Fed. Rep. of Germany

Received 22 July 1987; accepted for publication 4 November 1987

We report here on thermodynamic studies of Xe adsorption on Pt(111) using high resolution He scattering. From the data we extracted isosteric heats, partial molar entropies and lateral compressibilities in the adsorbed layer. Near completion of the commensurate $(\sqrt{3} \times \sqrt{3})$R30° phase, i.e. at the commensurate–incommensurate phase transition, we observe a substantial drop in the heat of adsorption of about 30 meV and an increase in the entropy of the adsorbed layer. The difference in adsorption heat $\Delta q_{st} \approx 30$ meV between the commensurate and the relaxed uniaxially compressed incommensurate phase reflects the binding energy difference between the lowest energy level occupied by the Xe atoms in the commensurate phase and the average of the energies of the sites occupied in the incommensurate phase; thus, Δq_{st} is a lower bound for the lateral corrugation of the substrate holding potential. The increase of the entropy of the adlayer in the incommensurate phase may be attributed to intrinsic properties of this phase. The results are discussed, and compared with recent Xe-adsorption studies on Ag(111) and Pd(100).

1. Introduction

We consider a monolayer of atoms adsorbed upon a periodic substrate. At temperatures, which are comparable or smaller than the characteristic energies of vertical excitations of the adsorbate, the adlayer represents a quasi-two-dimensional system. Physisorbed monolayers of rare gases on the basal plane of graphite and on single crystal metal surfaces provide experimental realization of such quasi-two-dimensional (2D) model systems, and thus receiving much interest [1]. The 2D adlayers can exist in several phases, some of which have their counterpart in 3D systems but some of them have no analogues in bulk matter.

The monolayer of xenon adsorbed on the (111) face of platinum appears to be one of the most interesting representatives of these quasi-2D systems [2–7]. At least six different phases have been observed so far. The corresponding schematic phase diagram in the temperature–coverage plane is shown in fig. 1. The coverage θ_{Xe} is defined here with respect to the density of Pt atoms in the (111) substrate surface, i.e. $\theta_{Xe} = 1$ corresponds to 1.5×10^{15} Xe atoms/cm^2.

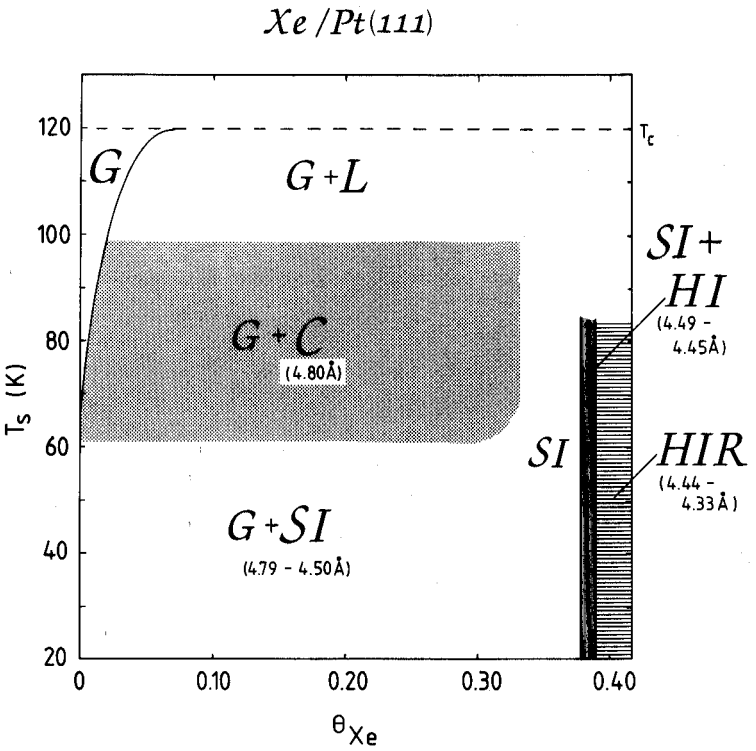

Fig. 1. Schematic phase diagram of Xe on Pt(111). C, SI, HI and HIR denote the commensurate $(\sqrt{3} \times \sqrt{3})$R30°, the striped incommensurate, the hexagonal incommensurate and the hexagonal incommensurate rotated 2D solid phases. G and L denote the 2D gas and liquid, respectively.

For coverages $\theta_{Xe} \lesssim 0.33$ and surface temperatures 62 K $\lesssim T_s \lesssim$ 99 K a $(\sqrt{3} \times \sqrt{3})$R30° commensurate phase (C) exists. At completion of the commensurate phase at $\theta_{Xe} \approx 0.33$ or by cooling down the adlayer below about 62 K the commensurate phase transforms in a continuous transition into a striped incommensurate phase (SI) [6]. In this striped phase, the Xe layer is uniaxially compressed along the $\bar{\Gamma}\bar{M}_{Xe}$ direction. Upon further increase of the adlayer density the striped phase (SI) transforms into a hexagonal incommensurate phase (HI) at coverages $\theta_{Xe} \gtrsim 0.38$. The HI-phase displays a continuous transition from a R30° to a rotated R30° ± 3.3° orientation (HIR) upon further coverage increase ($\theta_{Xe} \gtrsim 0.39$) [7].

Why is this particular adsorbate–substrate system so interesting? First, because the Xe monolayers adsorbed on the Pt(111) surface have the remarkable property to exhibit in (every) detail the theoretically predicted feature of the commensurate–incommensurate (CI) phase transition in two dimensions [8,9]. Indeed, the present understanding of the CI-transition, one of the

theoretically most thoroughly investigated phase transitions, is based on the assumption that the slightly incommensurate phase looks like an array of commensurate domains, separated by dense domain walls. It is the creation of these walls which drives the CI-transition. The wall concept leads to stringent predictions concerning the nature of the CI-transition. These may be summarized by quoting Villain [10]: "Conclusion: either the CI-transition is of first order or the hexagonal symmetry is destroyed near the transition". Xe on Pt(111) appears to be the first adsorption system fully consistent with the Bak–Mukamel–Villain–Wentowska theory (BMVW) [7,12]: Upon increasing the chemical potential, the commensurate $\sqrt{3}$ structure undergoes an uniaxial compression along the $\overline{\Gamma}\overline{M}$ azimuth; this symmetry breaking CI-transition is continuous, with the incommensurability following a power law with a critical exponent $\beta = 1/2$ [6]. Until very recently, there was no well established experimental confirmation of this prediction. On the contrary, the most intensively studied experimental system, Kr on graphite, exhibits apparently a continuous transition while hexagonal symmetry is preserved [11].

Second, and this seems to be an even more basic point, the mere existence of different solid Xe phases (C, SI, HI and HIR) on such a "smooth" surface like the (111) face of platinum is rather surprising. The various solid phases of rare gas adlayers on crystal surfaces arise as a result of competing interactions; lateral adatom versus adsorbate–substrate interactions.

The structure of the solid layer is determined ultimately by the delicate balance between the tendency of the adatoms to keep their natural lattice parameter and structure and the (differing) periodicity which the substrate tries to impose via the corrugation of the adatom–substrate interaction potential. The amplitude of the latter depends on the variation of the adsorption energy within the substrate unit cell (hollow, bridge or on top site). These periodic potential modulations of the "smooth", close packed single crystal metal surfaces have for a long time been assumed to be almost negligible. This assumption seems to be supported by adsorption experiments on Ag(111). In an impressive series of experiments Webb and coworkers [13–15] have been able to show that the properties of adsorbed monolayers of Xe, Kr and Ar on Ag(111) to a good approximation can be described by assuming a laterally uniform holding substrate potential. However, the existence of a commensurate Xe structure with a lattice parameter differing from the Xe natural one by nearly 10% and the occurrence of phenomena like registry–disregistry transitions and rotational ordering in Xe monolayers on the likewise close packed Pt(111) surface casts a new light on the role played by the lateral potential modulations of "smooth" metal surfaces. Black and Bopp [16] have recently investigated the Xe/Pt(111) system by molecular dynamics techniques. Unfortunately, the potential corrugation used in this calculation has been assumed to be so small, that even the existence of the commensurate $(\sqrt{3} \times \sqrt{3})R30°$ structure could not be reproduced, simply because the natural

lattice parameters $d_{Xe} = 4.39$ Å and $\sqrt{3}\, x d_{Pt} = 4.80$ Å are too much (8.6%) appart. On the other hand, this structure has been proved to be stable in an extended coverage and temperature range (see fig. 1).

The main goal of this paper is to provide thermodynamical data in order to facilitate realistic estimates of ranges for the "attractive" corrugation of the Xe/Pt(111) system. In section 2 we describe briefly our experimental procedure and in section 3 we report the thermodynamic adsorption properties as a function of coverage and measurements of the film compressibility in the uniaxially compressed incommensurate phase. The paper is closed with a discussion in section 4.

2. Experimental

The high resolution He scattering spectrometer used in these experiments has been described in detail recently [17]. The features pertinent to the present experiment are only briefly summarized here.

The sample is a high quality Pt(111) surface with an average terrace width of about 3000 Å (i.e. defect density less than 0.1%) [18]. The crystal is located in an ultrahigh vacuum chamber, with a base pressure in the low 10^{-11} mbar range. It is mounted on a manipulator that allows independent polar and azimuthal rotation and tilting. The temperature of the crystal can be regulated in the range $25 < T_s < 1800$ K. The temperature is measured with a chromel–alumel thermocouple, spot-welded to the crystal. It is calibrated in situ via the measurement of the Xe 3D vapor pressure. (Surface phonon spectroscopy is used to detect multilayer condensation [5,17].) The absolute accuracy of the temperature reading in the range of the present experiments is within ± 1 K.

The measurements are performed at a fixed total scattering angle, $\vartheta_i + \vartheta_f = 90°$. The angular spread of the incident beam and the angle subtended by the ionizer opening of the detector are both equal to 0.2°, i.e. the full instrumental angular resolution is $\leq 0.3°$. The measurements have been performed with a liquid nitrogen cooled nozzle, generating a 18.3 meV ($\lambda = 1.062$ Å) He beam with an energy spread $\Delta E = 0.25$ meV ($\Delta\lambda/\lambda = 0.007$).

Depending on the surface temperature the experiments have been performed under two different conditions. At higher temperature the Xe monolayers were studied in quasi-equilibrium with an ambient 3D Xe pressure ("quasi" because the 3D Xe was always at room temperature). These experiments will be referred to here as equilibrium experiments. For $T_s \lesssim 60$ K the equilibrium pressure being below 1×10^{-10} mbar, the ambient 3D Xe pressure cannot be monitored properly. Instead, Xe was adsorbed from the gas phase at pressures around 10^{-8} mbar and, when the desired coverage was reached, the 3D Xe gas was pumped off. In view of the very low desorption rate in this

temperature range, the fraction of the Xe atoms desorbing during the subsequent experiment is negligible, i.e. the absence of the ambient 3D Xe pressure has no influence on the Xe layer properties.

3. Results

3.1. Isosteric heat and partial molar entropy of adsorption

The isosteric heat of adsorption is obtained using the Clausius–Clapeyron equation:

$$\left.\frac{\partial \ln p}{\partial T}\right|_{\theta} = \frac{q_{st}}{kT^2}. \tag{1}$$

For many cases, the isosteric heat is independent of temperature, and q_{st} can be deduced from the slope of a semilogarithmic plot of ln p versus $1/T$ at constant coverage. Strictly speaking, the Clausius–Clapeyron equation is only valid if the chemical potentials in the 3D gas phase and in the surface layer are equal; this is not the case here because the 3D gas and the surface are at different temperatures, T_g and T_s respectively. It was shown by Ehrlich [19] that kinematical corrections can account for this temperature difference. In the case of Xe/Pt(111) this correction term is significantly smaller than the experimental uncertainty and can thus be disregarded.

The isosteres, i.e. ln p versus $1/T_s$ plots at θ_{Xe} = constant, have been measured in three different ways, depending on the coverage range:

3.1.1. $\theta_{Xe} \lesssim 0.03$, and $T_s > 70$ K, i.e. 2D gas phase

The specular He peak height scattered from a 2D lattice gas of adparticles is an unequivocal, extremely sensitive function of the adparticles coverage [20,21]. Thus, in the whole range where Xe is distributed like a 2D gas (θ_{Xe} low enough and T_s large enough), the isosteres are monitored by maintaining the relative specular He peak height I/I_0 = constant when varying the 3D Xe pressure and the surface temperature (I_0 is the peak height at $\theta_{Xe} = 0$; by taking I/I_0 the Debye–Waller effect is corrected for). The value of θ_{Xe} associated with each isostere is obtained in a good approximation from $\theta_{Xe} \simeq -\ln(I/I_0)/n_s\Sigma_{Xe}$, where Σ_{Xe} is the scattering cross section for diffuse scattering per Xe adatom and n_s the density of adsorption sites.

3.1.2. $0.04 \lesssim \theta_{Xe} \lesssim 0.33$, and $62\ K < T_s < 99$ K, i.e. 2D-gas and commensurate solid phase

The height of any one of the He diffraction peaks (except the specular one) is a good measure of the number (normalized to the number of Pt atoms) θ_{Xe}^{c} of the Xe adatoms which make up the $\sqrt{3}$ commensurate islands; i.e. a correct measure as soon as the islands are large compared to the instrumental transfer

width. The constancy of the number of Xe atoms in the $\sqrt{3}$ commensurate islands is ensured by keeping the height of the $(2, 2)_{C-Xe}$ diffraction peak constant. Accordingly, the isosteres have been obtained by plotting ln p_{3DXe} versus $1/T_s$ at constant peak height, which has been corrected for Debye–Waller effects.

3.1.3. $0.33 < \theta_{Xe} \leq 0.38$, i.e. striped incommensurate solid phase

The striped incommensurate phase which results by increasing θ_{Xe} above the commensurate layer completion at $\theta_{Xe} = 0.33$ is a compression phase. Its lattice constant d^I_{Xe} is a good measure of the density whithin the incommensurate domains. By assuming that the number of defects and disordered atoms does not depend on T_s, the plots ln p_{3DXe} versus $1/T_s$ at constant d^I_{Xe} represent true isosteres. The reproducibility and consistency of the results obtained at various d^I_{Xe} shows that the assumption is fairly correct.

In fig. 2 we plot the isosteric heat of adsorption q_{st}, obtained in the manner described above, as a function of coverage. The initial heat of adsorption ($\theta_{Xe} = 0.005$) is 277 meV; it increases steadily to about 312 meV at $\theta_{Xe} = 0.33$. This continuous increase is indicative of attractive mutual interactions. Upon further increase of the Xe coverage, $\theta_{Xe} > 0.33$ (CI-transition), a substantial drop in q_{st} to a value of ~ 280 meV is observed.

Quasi-equilibrium measurements also give access to the partial molar entropy in the adsorbed Xe layer, according to [22]:

$$\tilde{S}_{ad} = -q_{st}/T_s - k \ln(p/p_0) + S^0_g, \tag{2}$$

where $\tilde{S}_{ad}$ is the partial molar entropy of the adsorbed layer, S^0_g the molar entropy of gaseous Xe at a pressure p_0 and temperature T_g, k the Boltzmann constant = 0.08161 meV K^{-1}, p the equilibrium pressure of the 3D Xe gas, T_s the surface temperature and p_0 the reference pressure (usually chosen to be 1

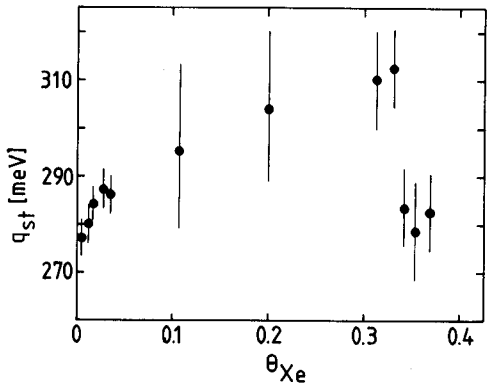

Fig. 2. Isosteric heat of adsorption q_{st} of Xe on Pt(111) as a function of coverage θ_{Xe}.

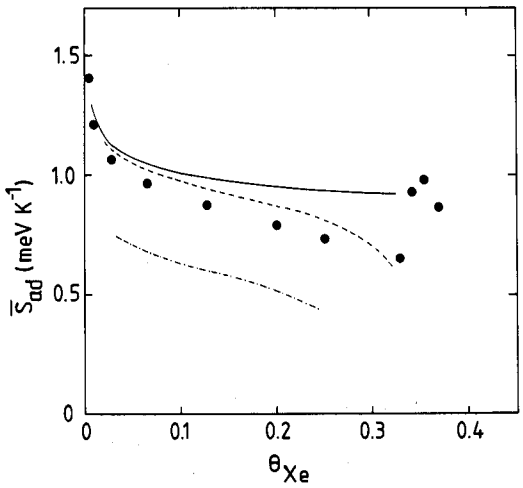

Fig. 3. Differential molar entropy of the Xe adlayer on Pt(111) as a function of coverage. The closed circles are the data points. They are compared with calculated entropy values assuming: (———) completely mobile 2D ideal gas, (— — —) completely mobile Volmer gas, and (·–·–·) localized adlayer. The vibrational entropies $\tilde{S}_{\perp}^{vib} = 0.16$ meV K^{-1}, $\tilde{S}_{\ell}^{vib} = 0.13$ meV K^{-1} and $\tilde{S}_{t}^{vib} = 0.16$ meV K^{-1} have been extracted from lattice dynamical studies [3,54].

atm). The last two terms on the right-hand side of eq. (2) constitute the entropy of the 3D gas at equilibrium, while q_{st}/T_s accounts for the entropy loss of the gas upon adsorption. In the case of a monoatomic gas, like Xe, the molar entropy of the gas phase, S_g^0, is just the translational entropy, which can be calculated after the Sackur–Tetrode equation [23].

The partial molar entropy $\tilde{S}_{ad}$ is plotted as a function of coverage in fig. 3. The data were obtained from an equilibrium isotherm taken at $T_s = 93.5$ K. A continuous decrease of the partial molar entropy is observed in the range $0 < \theta_{Xe} < 0.33$; the total decrease is about 0.8 meV K^{-1}. At the CI-transition a substantial increase of the partial molar entropy by more than 0.3 meV K^{-1} occurs.

3.2. Thermal expansion coefficients

$\overline{\Gamma}\overline{\mathrm{M}}$ uniaxial expansion coefficients of the fully relaxed striped incommensurate Xe layers on Pt(111) (misfit range 4.5–6.5%, no wall effects) [24] have been obtained by measuring the Xe lattice constant $d_{Xe}^{\overline{\Gamma}\overline{\mathrm{M}}}$ in the $\overline{\Gamma}\overline{\mathrm{M}}$ azimuth as a function of temperature. The measurements have been performed for unconstrained layers ($\theta_{Xe} < 0.33$ and $T_s < 60$ K, i.e. at negligible spreading pressure, $\varphi \approx 0$). In fig. 4a we show the variation of the Xe lattice constant $d_{Xe}^{\overline{\Gamma}\overline{\mathrm{M}}}$ of the unconstrained incommensurate Xe layer as a function of temperature. The unconstrained monolayers were prepared by dosing the surface with

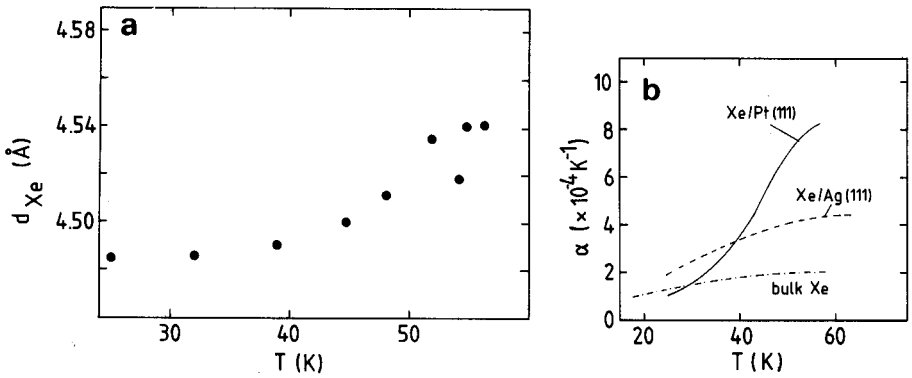

Fig. 4. (a) Variation of the Xe lattice constant $d_{Xe}^{\Gamma M}$ of the unconstrained Xe monolayer with temperature in the misfit range 4.5%–6.5%. (b) Linear thermal expansion coefficient α of the unconstrained monolayer calculated from the data in fig. 4a. Also shown is the value for bulk Xe (·–·–·) and for Xe monolayers on Ag(111) (— — —) [13].

Xe at 25 K up to various $\theta_{Xe} < 0.33$ and then annealing the layer. No dependence of the lattice constant on the coverage at constant T_s was observed in the range $0 < \theta_{Xe} \lesssim 0.33$. The thermal expansion coefficient of the unconstrained monolayer is defined by:

$$\alpha = \left(d_{Xe}^{\Gamma M}\right)^{-1} \left(\partial d_{Xe}^{\Gamma M}/\partial T\right)_{\varphi=0}. \tag{3}$$

The coefficient α calculated from the data points in fig. 4a is plotted in fig. 4b as a function of temperature. Also included for comparison are thermal expansion coefficients of bulk Xe and for Xe adsorbed on Ag(111) [13].

For an ideal gas in equilibrium with a 2D adsorbed phase of area b per adatom the 2D isothermal compressibility is defined as:

$$K_T = -(1/kT)(\partial b/\partial \ln p)_T. \tag{4}$$

In fig. 5a we show the variation of the xenon lattice parameter $d_{Xe}^{\Gamma M}$ at $T = 88$ K as a function of 3D Xe equilibrium pressure and in fig. 5b the deduced values of the isothermal compressibility. For comparison we also plot the values of K_T obtained by Unguris et al. for Xe adsorption on Ag(111) [15] as well as a theoretical curve for an ideal two-dimensional van der Waals film using the Barker X2-potential [25].

The various compressibility coefficients are always somewhat larger than expected for an ideal two-dimensional film fully governed by the lateral forces between the adatoms as they move in a laterally flat holding substrate potential, for which Xe on Ag(111) might be a good representative. This result is not unexpected, since the binding energy as well as the lateral potential

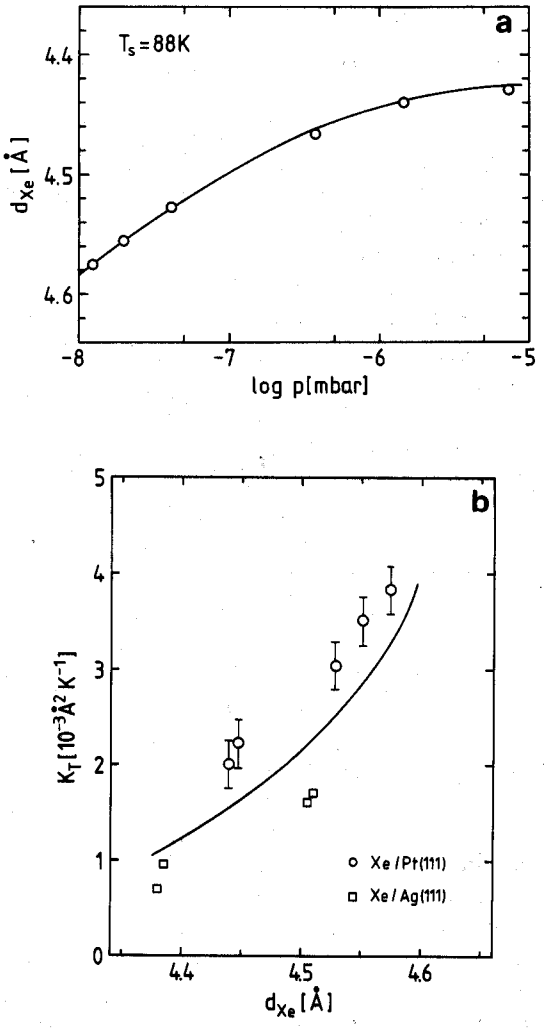

Fig. 5. (a) Variation of the Xe lattice constant $d_{Xe}^{\Gamma M}$ with Xe vapor pressure at $T = 88$ K. (b) Isothermal lateral compressibility of Xe/Pt(111) (○) as a function of lattice constant, calculated from the data in fig. 5a. Also shown are the compressibility of a model 2D Xe layer using the Barker X2 potential (———) and experimental values of Xe/Ag(111).

corrugation for Xe is about 30% larger on Pt(111) than on Ag(111) (see below). It is well known that the tendency for compression is larger on strong substrates [26]; this compression arises from the large gradient of the substrate–adatom attraction.

4. Discussion

4.1. Adlayer structure and the corrugation of the holding potential

The most remarkable point in the variation of the isosteric heat with coverage is the substantial drop at coverages above $\theta_{Xe} = 0.33$. At densities less than $\theta = 0.33$, the xenon atoms form a $(\sqrt{3} \times \sqrt{3})R30°$ commensurate solid in registry with the platinum substrate lattice. All Xe atoms sit in the same type of energetically most favorable adsorption sites (probably the three-fold hollow sites). At densities exceeding a full commensurate monolayer ($\theta_{Xe} > 0.33$) and due to the size of the Xe atoms, it is no longer possible for all Xe atoms to occupy the energetically most favorable adsorption sites; extra atoms are accommodated in dense "domain walls" separating commensurate domains. These extra adatoms populate interstitial lattice sites, e.g. bridge and on top positions, which are energetically less favourable. The existence of a striped domain structure (SI) of broad superheavy walls (~ 6 interrow distances FWHM) in the Xe/Pt(111) system in a very narrow coverage range ($0.33 < \theta_{Xe} < 0.345$) has been inferred recently from high resolution He diffraction studies [6]. Upon further increase of the coverage these domain walls strongly relax and the incommensurate layer (I) can be described in terms of a uniform uniaxial compression ($0.345 \lesssim \theta_{Xe} \lesssim 0.38$) in the $\overline{\Gamma}\overline{M}_{Xe}$ direction. In this uniaxially compressed layer the Xe atoms occupy all kind of sites corresponding to the entire range of binding energies between the strongest bound sites (probably three-fold hollow) and the less bound ones (probably on top). The propensity for stronger bound sites may be materialized into some extent by local relaxation. The substantial difference in q_{st} between the C and the uniaxially compressed incommensurate phase reflects the binding energy difference between the lowest energy level (of the strongest binding sites) occupied by the Xe atoms in the commensurate phase and the average of the energies of the sites occupied in the incommensurate phase. The value $\Delta q_{st} \approx 30$ meV is thus a reasonable measure of the average value of the corrugation of the holding potential. The actual value is probably somewhat larger because of the preferential occupation of stronger bound sites in the I-phase and because the lateral Xe–Xe binding energy in the I-phase is slightly larger than in the C-phase (the Xe lattice constant in the I-phase being nearer to the "natural" Xe lattice constant than in the C-phase).

A value of 30 meV for the average corrugation of the holding potential in the Xe/Pt(111) system is supported by recent photoemission studies of Schönhense et al. [29,30]. It was shown by Wandelt and coworkers [31,32] that the electronic binding energy of valence and core levels of adsorbed layers of noble gases is independent of the substrate when referred to the local vacuum level. Thus, it has to be expected that Xe atoms located further away from the surface (e.g. in bridge or top sites), i.e. at a higher local potential, lead to lower

electronic binding energies than Xe atoms located closer (e.g. in three-fold hollow sites), i.e. at a lower local potential.

Upon increasing the coverage above that of the commensurate $\sqrt{3}$ phase Schönhense et al. [29,30] observed a systematic shift of the $5p^{1}_{3/2}$ and $5p^{3}_{3/2}$ levels towards lower binding energy by roughly 0.4–0.5 eV, indicative for a population of adsorption sites located further away. Lang [33] has calculated the dependence of the local potential shift on the Xe substrate distance within the charge density formalism, using a jellium model. According to this calculations, the observed valence orbital shift of 0.5 eV towards lower binding energies corresponds to a vertical separation of about 0.3 Å between the adsorption sites in the commensurate and in the uniaxially compressed phase. This outward shift corresponds to a reduction of the binding energy of roughly 10%, i.e. again about ~ 30 meV, in agreement with the value obtained above.

The size of the average lateral corrugation of the attractive part of the Xe/Pt(111) potential of ~ 30 meV = 350 K, as deduced above from thermodynamic and photoemission data seems to be surprising in view of the widespread believe that for rare gases adsorbed on close packed metal surfaces this corrugation is negligible.

This belief originates in the very low corrugation of the interaction potential as deduced from the He diffraction patterns from close packed metal surfaces. To infer from this that the lateral corrugation felt by *all* rare gases *adsorbed* on close packed metal surfaces is negligible is at least risky. Indeed, in diffraction experiments the He atoms probe the corrugation of the repulsive interaction potential in the region of positive energies, while adsorbed atoms feel the corrugation of the bottom of the attractive potential well. On the other hand, the interaction of heavier rare gases like Xe, Kr or even Ar differs appreciably from the interaction of He with the same substrates. (It is interesting to mention in this context that the corrugation of the repulsive potential as deduced from Ne diffraction experiments is substantially larger than in the case of He [36].) As already noted in the introduction, the molecular dynamics calculation of Black and Bopp [16] indicates also that by assuming a corrugation amplitude of the holding potential of only 25 K bridge–hollow ($V_B - V_H$) and 165 K on top–hollow ($V_T - V_H$), the experimentally well established $\sqrt{3}$ commensurate Xe structure on Pt(111) cannot be reproduced. It is certainly not only the largest amplitude of the corrugation ($V_T - V_H$) which determines the results of the calculation, but also the overall shape of the potential. In particular, the value of the potential at the bridge site, V_B, which determines ultimately the height of the diffusion barrier ($V_B - V_H$), is of importance. It seems that the potential chosen by Black and Bopp underestimates this value when compared with Steele's potential [35] which has been found to be appropriate in describing numerous adsorbate–substrate systems; indeed, the value of the ratio $(V_B - V_H)/(V_T - V_H)$ is strongly different for the two potentials: about 1/7 and 8/9, respectively.

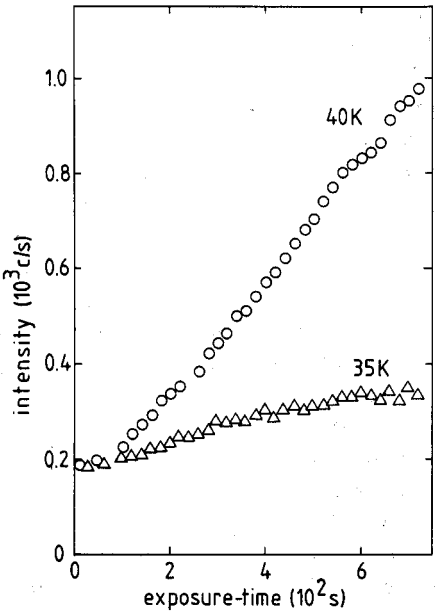

Fig. 6. Diffraction peak height of the (1, 1)-peaks versus Xe exposure time at constant temperature: (a) 40 K, (b) 35 K.

The diffusion barrier for Xe on W(110) – which is also a rather close packed surface – has been measured directly by Chen and Gomer [37] by means of the field emission current fluctuation method. They found a value of ~ 47 meV = 545 K, consistent with the value obtained above for Xe/Pt(111). Additional support comes from a recent high resolution He diffraction study of the Kr/Pt(111) system [38], which forms a high order commensurate locked phase at higher coverages. Although, here only every sixth Kr atom is found to be located in a three-fold hollow site, this phase is found to be efficiently locked in a temperature range of at least 25 K.

An additional cross-check for the value of the diffusional barrier may come from the observation of mobility effects of the adsorbed Xe. It is generally supposed that a crossover from mobile to immobile adsorption takes place somewhere at a temperature $T_{\mathrm{IM-M}} \approx E_{\mathrm{diff}}/10k$ [39], where k is the Boltzmann constant and E_{diff} the diffusional barrier for migration between adjacent sites. The growth of the incommensurate Xe phase during Xe adsorption ($p_{\mathrm{Xe}} = 8 \times 10^{-9}$ mbar) at two constant temperatures is exemplified in fig. 6. The growth is followed by monitoring the peak height of the $(1, 1)_{\mathrm{Xe}}$ diffraction peak versus exposure-time. In fig. 6a the temperature was $T = 40$ K; after a short induction period the peak height increases almost linearly with

exposure [2]. A detailed analysis of the peak profiles shows that the average island size increases almost linearly with coverage; the average domain size at exposures of 700 s is about 150 Å. This behaviour characterizes the condensation of mobile adsorbates. In fig. 6b the temperature was $T = 34$ K; here the diffraction peak height increases only slightly with exposure. Peak profile analysis shows that islands with an average domain size of only ~ 30 Å are formed, nearly independent of exposure; a behavior characteristic for condensation of nearly immobile adsorbates. From the results of fig. 6 we can infer that for Xe on Pt(111) there exists a mobile–immobile transition somewhere between 30 and 40 K, again in fair agreement with the magnitude of the diffusional barrier deduced above from the isosteric heat data.

4.2. Interactions within the Xe adlayer versus substrate nature

A comparison between the behavior of the Xe adlayer on Pt(111) as described above (commensurate island formation, C–SI phase transition, etc.) and the behavior of Xe adlayers on other substrates like Ag(111) and Pd(100) is particularly interesting, even if not yet fully understood.

Xe adsorption on Ag(111) was extensively studied by Webb and coworkers [13–15]. It has been found that Xe/Ag(111) is an island forming system. However, in contrast to Xe/Pt(111), the effect of the corrugation of the holding potential is very weak: only the azimuthal orientation of the hexagonal Xe adlayer is correlated with that of the Ag(111) substrate (it is aligned within a few degrees), while its lattice constant is always incommensurate with that of the substrate. One of the main conclusions was that "to a very good approximation it appears that the gases are adsorbed on a smooth dielectric continuum. Thus the properties of the adsorbed phases are governed by the lateral forces between the adatoms as they move in the laterally uniform holding potential due to the substrate" [13].

Xe adsorption on Pd(100) has been studied by Wandelt and coworkers [40,41] and by Moog and Webb [42]. One of the most prominent findings related to the comparison here is the lack of any diffraction feature below monolayer saturation; there is no evidence for island formation down to 10 K. Thus, Xe on Pd(100) appears to be governed by repulsive lateral adatom interactions, only.

Thus, with the adsorption systems Xe/Pt(111), Ag(111), Pd(100) we have three systems, behaving totally different:

Xe/Pt(111): Xe–Xe attractive interactions (island forming system), *pronounced* registry effects;

Xe/Ag(111): Xe–Xe attractive interactions (island forming system), *no* registry effects;

Xe/Pd(100): Xe–Xe repulsive interactions.

Table 1

	q_{st} ($\theta_{Xe} \to 0$) (meV)	$\Delta\phi$ (meV)	$\bar{\mu}$ (D)	ΔE_B ($5p_{3/2}$) (meV)	θ_{crit} (% ML)
Ag(111)	215 [15]	480 [32]	0.2 [32]	~ 500 [32]	6 [47]
Pt(111)	277 [5]	~ 600 [45]	–	~ 580 [29]	~ 1–2 [20]
Pd(100)	273 [42]	~ 700 [42]	0.36 [40]	~ 520 [46]	100 [40]

The most puzzling substrate effect is the difference between Pt and Ag on one side (island formation) and Pd on the other (2D gas up to monolayer saturation). In their original work Miranda et al. [40] ascribed the discrepancy to a strong reduction of the Xe nearest-neighbor attraction due to substrate induced repulsive interactions between Xe adsorbed on Pd. However, these repulsive contributions, which have been calculated by Bruch [42,43] to be ~ 30, 20.2 and 20.3 meV for Pt, Ag and Pd, respectively, are substantially smaller than the Xe–Xe attractive interaction of 77 meV and in addition larger for Pt than for Pd. Thus, these interactions cannot account for the dramatic difference in the behavior of the three metals.

In a very recent paper, Jabłonski et al. [44] proposed an empiric correlation for the tendency to form islands. This tendency should be more pronounced the lower the adsorption energy, the larger the dipole moment per Xe atom and the smaller the adsorption induced splitting of the $5p_{3/2}$ valence level. The physical properties of Xe adsorption on these three metals are summarized in table 1. Obviously the trend proposed by Jabłonski et al. fails for the three metals considered here. The adsorption energy is nearly equal for Pt(111) and Pd(100), and about 30% larger than on Ag(111). The adsorption induced valence orbital splitting is the largest for Pt, while for Ag only slightly smaller than for Pd. Though the Xe dipole moment $\bar{\mu}$ for adsorption on Pt(111) is not explicitly known, it is expected to have a similar value as on Pd(100), as indicated by the nearly equal work function change, $\Delta\phi$.

Since the substrate mediated repulsive forces cannot account for the difference between Pd and Ag/Pt one has to look for some additional mechanism. Based on the jellium calculations of Lang, Moog and Webb [42] suggested that the deformation of the substrate electron density distribution by the adsorbed Xe atom might give rise to an additional repulsive contribution to the lateral adatom interaction. This deformation of the electron charge distribution should be more pronounced for a d-metal like Pd, with its large density of states near the Fermi level [48], than for the s-metal Ag. Unfortunately this argument cannot explain the difference between Pd and Pt, because Pt has a high density of states at the Fermi level as well [49].

The arguments we have used so far without particular success to understand the obvious differences in the Xe adlayer behavior due to the substrate nature were mainly confined to "physical" interactions. If we take the heat of

sublimation of bulk Xe (171 meV) as a measure of pure "physical" dispersion forces, the isosteric heates of adsorption of Xe on Pd and Pt (table 1) contain a "chemical" contribution of roughly 40%; for Ag, this "chemical" part is more than twice smaller. This "chemistry" effect, involving directed bond interactions between adatom and substrate, seems to be reflected in photoemission measurements. Upon adsorption of Xe on Pt(111) Eyers et al. [50] observed the emergence of a new peak 0.25 eV below the Fermi energy, which does not show any dispersion for different coverages of Xe. This effect has also been observed for Xe adsorption on various Pd surfaces [41], and has been considered as direct indication for chemical bond formation between Xe and the metal surface [51]. If chemical bonding effects are as important as it seems, cluster calculations of Xe adsorption on Pt and Pd, including direct bond interactions, appear to be the right way to uncover the origin of the substantial difference in the adlayer behavior induced by these metals. Indeed, in complex-chemistry it is well known that substantial differences in the behavior of Pt and Pd do exist [52].

The difference in the behavior of Xe on Ag(111) and Pt(111) is certainly less dramatic: in both cases Xe islands are formed at submonolayer coverage, because the Xe–Xe interaction is attractive. However, while the Xe adlayer on Ag(111) is always incommensurate, on Pt(111) obvious registry–disregistry effects occur, dominated by the existence of the $\sqrt{3}$ commensurate structure, which is stable in an extended coverage range. In addition, no reduction of Xe mobility down to 25 K has been observed on Ag(111) [13], while on Pt(111) the mobility is strongly reduced below 35 K (see above). These differences can be reasonably understood in view of the ~ 30% larger binding energy of Xe on Pt than on Ag and of the smaller lattice constant of Pt compared to that of Ag (3.92 and 4.09 Å, respectively). The ratio of the temperatures at which the Xe adatoms become immobile is related to the ratio of the binding energies, if we make the assumption that the barrier for diffusion scales with the binding energy. The explanation for the differences in the structure of the Xe layer is also straigthforward. The $\sqrt{3}$ commensurate Xe adlayer on Pt(111) is appreciably strained. Indeed, the misfit between the "natural" nearest neighbor Xe distance (4.39 Å at 65 K) and the nearest neighbor distance in the $\sqrt{3}$ commensurate Xe layer (4.80 Å $= \sqrt{3}\, d_{\mathrm{Pt}}$) is ~ 9%. For a $\sqrt{3}$ commensurate Xe layer on Ag the misfit would be larger than 13% and thus the strain energy to be compensated more than two times larger. The corrugation amplitude of the Xe/Ag(111) potential being ~ 30% smaller, the absence of registry effects on Ag(111) is not unexpected.

4.3. Entropy of the adsorbed layer

Additional insight in the properties of the adsorbed Xe layer on Pt(111) can be obtained by comparing the experimental data shown in fig. 3 with entropies

calculated from simple statistical mechanics models [53], namely, mobile 2D ideal gas (——), mobile Volmer gas (— — —), and localized adsorption (·–·–·). At low coverages, the data are in good agreement with the model calculations of delocalized adsorption. With increasing coverage, the experimental data are best described by the Volmer model; neither the ideal 2D gas model nor the localized model is consistent with the data. In particular, the localized model calculations predict in the entire coverage range entropy values which are much to low. This suggest a high mobility of the Xe layer, in accordance with experimental findings.

Of particular interest in the experimental entropy data is the obvious increase at coverages just above $\theta_{Xe} = 0.33$. As already noted, at this coverage the Xe monolayer on Pt(111) undergoes a commensurate–incommensurate transition. In a very narrow coverage range (see above) the weakly incommensurate Xe phase can be considered as an array of commensurate domains separated by broad incommensurate domain walls. At temperatures $T > 0$ K domain walls may slightly deviate from their easy directions, and the walls meander. These irregularities of the superstructure produces some extra entropy. This effect, however, is small; in an otherwise ordered monolayer the entropy gained is at maximum $S = k \ln 2$, a value much to small to account for the observed increase.

A basic property of a commensurate locked layer is that it has discrete rather than continuous symmetry, i.e. infinitesimal displacements of the whole layer costs a non-zero amount of energy. Due to this broken translational invariance the longitudinal phonon branches have finite frequencies at the zone center, i.e. there exist no acoustical phonon modes. In the incommensurate phase, however, the reestablished translational invariance allows also for acoustical modes. Because there are no calculations of the phonon gap in the density of states of commensurate layers we cannot give a realistic estimation of its contribution to the entropy of the adlayer. A very rough estimation may be still obtained by considering the low frequency optical modes of the collective longitudinal and transversal motions of the domain walls. Since the frequency of these phonons is quite low, they contribute significantly to the entropy of the monolayer in the weakly incommensurate phase. Shrimpton, Bergersen and Joos [55] have calculated recently the phonon dispersion of the domain wall modes for krypton monolayers on graphite. (It is certainly not clear whether these results can be applied to the broad walls of Xe on Pt.) Depending on the values used for the graphite potential corrugation they obtained frequencies $h\nu = 0.02$–0.1 meV for the lowest lying modes. Since the vertical phonon frequencies for Kr/graphite and Xe/Pt(111) are not very different, we may use these values to estimate the entropy contribution of the wall excitations. Taking for instance $h\nu = 0.05$ meV we obtain an entropy increase at the commensurate–incommensurate transition of 0.46 meV K^{-1}, i.e. of the right order of magnitude.

References

[1] S.K. Sinha, Ed., Ordering in Two Dimensions (North-Holland, Amsterdam, 1980).
[2] K. Kern, R. David, R.L. Palmer and G. Comsa, Phys. Rev. Letters 56 (1986) 620.
[3] K. Kern, R. David, R.L. Palmer and G. Comsa, Phys. Rev. Letters 56 (1986) 2823.
[4] K. Kern, R. David, R.L. Palmer and G. Comsa, Appl. Phys. A41 (1986) 91.
[5] K. Kern, R. David, R.L. Palmer and G. Comsa, Surface Sci. 175 (1986) L669.
[6] K. Kern, R. David, P. Zeppenfeld, R.L. Palmer and G. Comsa, Solid State Commun. 62 (1987) 391.
[7] K. Kern, Phys. Rev. B35 (1987) 8265.
[8] J. Villain and M.B. Gordon, Surface Sci. 125 (1983) 1.
[9] P. Bak, in: Springer Series in Chemical Physics, Vol. 35, Eds. R. Vanselow and R. Howe, (Springer, Berlin, 1985) p. 317.
[10] J. Villain, in: Ordering in Two Dimensions, Ed. S.K. Sinha (North-Holland, Amsterdam, 1980).
[11] P.W. Stephens, P.A. Heiney, R.J. Birgeneau, P.M. Horn, D.E. Moncton and G.S. Brown, Phys. Rev. B29 (1984) 3512.
[12] P. Bak, D. Mukamel, J. Villain and K. Wentowska, Phys. Rev. B19 (1979) 1610.
[13] J. Unguris, L.W. Bruch, E.R. Moog and M.B. Webb, Surface Sci. 87 (1979) 415.
[14] L.W. Bruch, J. Unguris and M.B. Webb, Surface Sci. 87 (1979) 437.
[15] J. Unguris, L.W. Bruch, E.R. Moog and M.B. Webb, Surface Sci. 109 (1981) 522.
[16] J.E. Black and P. Bopp, Phys. Rev. B34 (1986) 7410.
[17] R. David, K. Kern, P. Zeppenfeld and G. Comsa, Rev. Sci. Instr. 57 (1986) 2774.
[18] B. Poelsema, R.L. Palmer, G. Mechtersheimer and G. Comsa, Surface Sci. 117 (1982) 62.
[19] G. Ehrlich, J. Chem. Phys. 36 (1962) 1499.
[20] B. Poelsema, L.K. Verheij and G. Comsa, Phys. Rev. Letters 51 (1983) 2410.
[21] B. Poelsema, L.K. Verheij and G. Comsa, Surface Sci. 152/153 (1985) 851.
[22] S. Cerny, in: The Chemical Physics of Solid Surfaces and Heterogeneous Catalysis, Vol. 2, Eds. D.A. King and D.P. Woodruff (Elsevier, Amsterdam, 1983) p. 1.
[23] L.K. Nash, Elements of Statistical Thermodynamics (Addison-Wesley, Reading, MA, 1973).
[24] In this misfit range domain wall effects play no role, since the layer can be considered as a fully relaxed uniaxially compressed phase, with the lattice parameter variation governed by thermal expansion.
[25] L.W. Bruch and J.M. Phillips, Surface Sci. 91 (1980) 1.
[26] D.A. Huse, Phys. Rev. B29 (1984) 6985.
[27] K. Kern, Jül-Report 2040, January 1986.
[28] M. Kardar and A.N. Berker, Phys. Rev. Letters 48 (1982) 1552.
[29] G. Schönhense, A. Eyers, U. Friess, F. Schäfers and U. Heinzmann, Phys. Rev. Letters 54 (1985) 547.
[30] G. Schönhense, Appl. Phys. A41 (1986) 39.
[31] J. Hulse, J. Küppers, K. Wandelt and G. Ertl, Appl. Surface Sci. 6 (1980) 453.
[32] R.J. Behm, C.R. Brundle and K. Wandelt, J. Chem. Phys. 85 (1986) 1061.
[33] N.D. Lang, Phys. Rev. Letters 46 (1981) 842.
[34] S. Raaen, M. Ruckmann and M. Strongin, Phys. Rev. B31 (1985) 623.
[35] W.A. Steele, Surface Sci. 36 (1973) 317.
[36] K.H. Rieder and W. Stocker, Phys. Rev. Letters 52 (1984) 352.
[37] J.R. Chen and R. Gomer, Surface Sci. 94 (1980) 456.
[38] K. Kern, P. Zeppenfeld, R. David and G. Comsa, Phys. Rev. Letters 59 (1987) 79.
[39] G. Ertl and J. Küppers, Low Energy Electrons and Surface Chemistry (Verlag Chemie, Weinheim, 1974).
[40] R. Miranda, S. Daiser, K. Wandelt and G. Ertl, Surface Sci. 131 (1983) 61.

[41] K. Wandelt and J. Hulse, J. Chem. Phys. 80 (1984) 1340.
[42] E.R. Moog and M.B. Webb, Surface Sci. 148 (1984) 338.
[43] L.W. Bruch, private communication.
[44] A. Jabłonski, S. Eder, K. Markert and K. Wandelt, J. Vacuum Sci. Technol. A4 (1986) 1510.
[45] B.E. Nieuwenhuys, D.Th. Meijer and W.M.H. Sachtler, Phys. Status Solidi (a) 24 (1974) 115.
[46] K. Horn, M. Scheffer and A.M. Bradshaw, Phys. Rev. Letters 41 (1978) 822.
[47] J. Unguris, L.W. Bruch, M.B. Webb and J.M. Phillips, Surface Sci. 114 (1982) 219.
[48] J.R. Gay, J.R. Smith, F.J. Arlinghaus and T.W. Capehart, Phys. Rev. B23 (1981) 1559.
[49] M.C. Desjonquères and F. Cyrot-Lackmann, Solid State Commun. 18 (1976) 1127.
[50] A. Eyers, G. Schönhense, U. Friess, F. Schäfers and U. Heinzmann, Surface Sci. 162 (1985) 96.
[51] J. Küppers, F. Nitschke, K. Wandelt and G. Ertl, Surface Sci. 87 (1979) 295.
[52] P. Qini et al., J. Am. Chem. Soc. 98 (1976) 7225; 101 (1979) 6110.
[53] A. Clark, The Theory of Adsorption and Catalysis (Academic Press, New York, 1970).
[54] J. Black, private communication.
[55] N.D. Shrimpton, B. Bergersen and B. Joos, Phys. Rev. B34 (1986) 7334.